



Investigation of The Rainwater Harvesting Potential at the Mersin University, Turkey

A. Yasin YİĞİT¹, Osman ORHAN^{*2}, Ali ULVİ²

¹Mersin University, Faculty of Engineering, Department of Geomatics Engineering, Mersin, Turkey

²Mersin University, Department of Remote Sensing & GIS, Mersin, Turkey

Keywords

Rainwater harvesting
UAV
Irrigation
Classification

ABSTRACT

The rapid population growth in the world and the adverse effects of climate change, has caused a severe increase in water demand used in sectors such as agriculture, industry, and domestic usage. The fact that the water resources in the world are stable and their availability is limited, the importance of water resources, efficient use of water, and the use of technologies related to alternative water resources have become important. This study aimed to investigate the usage potential of rainwater to be collected from the roofs of the building in irrigation of green areas in Mersin University - Çiftlikköy campus. For this purpose, first, whether the roofs inside the campus can collect rainwater will be revealed with unmanned aerial vehicles. Then, appropriate roof areas where rainwater will be collected will be calculated using the object-based classification method. The rainwater amounts to be collected from each building will be calculated using the monthly precipitation data obtained from the Provincial Directorate of State Meteorology Affairs. In addition, by calculating the number of green areas on the campus and the need for rainwater, it was determined how much rainwater to be collected meets the water need according to different irrigation periods.

1. INTRODUCTION

In general, greenhouse gases increase, and greenhouse gas effects are strengthened due to various human activities such as burning fossil fuels, land-use change, deforestation, such as. The increase in greenhouse gases in the atmosphere causes global warming and as a result, climate change occurs (Trenberth, 2011; Olaniyi et al., 2019). Recently, excessive, and unconscious use of resources has caused global warming, which has brought climate changes. Due to climate change, temperature increases and changes in precipitation regimes have come to the fore. Climate change: affects stream flows, groundwater, and water volumes in lakes depending on changes in temperatures and precipitation. This effect does not have a regular process; It causes a decrease in precipitation in winter, sudden precipitation in summer, and above or below seasonal temperature averages (Sandalcı, 2011).

Water, which is the main element of life, is a very effective substance not only in the living environment but also in the inanimate environment. Natural

phenomena such as the formation of soil by physically breaking the rocks, the fertility of the soil by dissolving the substances in it, the emergence of plants, the transportation of the necessary building blocks from the roots to the leaves on the branches, and photosynthesis take place through the water. "Life started in water". The proposition is indicative of the importance of water on earth. Although 97.5% of the world is covered with water, only 2.5% of this water is usable. Considering that 2% of this limited amount is found at the poles as ice masses of 16 km thickness, only 0.5% of the water is usable (Ulusoy, 2007).

When countries are classified according to water availability, countries with an average amount of usable water less than 1000 m³ per year are water-poor countries, countries with 1,000-3,000 m³ water shortages, countries with 3,000-10,000 m³ water, less than 10,000 m³. And the countries with high levels are considered water-rich countries (Alparslan et al., 2008; Şahin and Manioğlu 2011). The amount of water available per person per the year 1500-1600 cubic meters. Turkey is a country suffering from water shortages. Because Turkey's population is expected to

* Corresponding Author

(ayasinyigit@mersin.edu.tr) ORCID ID 0000-0002-9407-8022
*(osmanorhan44@gmail.com.tr) ORCID ID 0000-0002-1362-8206
(aliulvi@mersin.edu.tr) ORCID ID 0000-0003-3005-8011

Cite this article

Yiğit A Y, Orhan O & Ulvi A (2020). Investigation of The Rainwater Harvesting Potential at the Mersin University, Turkey. Mersin Photogrammetry Journal, 2 (2), 64-75

rise to 87 million over the next 20 years. With the increase in the population, it is estimated that the amount of water per person will decrease to 1042 cubic meters. In this case, in terms of the future, Turkey will be a candidate to be one of the most water-poor countries (Eren et al., 2016; SFR, 2017).

Studies have been conducted to examine the impact of climate change on hydrology by focusing on the water cycle and water resources on human and environmental water use. One of these studies is rainwater harvesting. Only 30% of rainwater is added to groundwater, and the remaining 70% cannot be utilized (Kılıç, 2008; Haddeland, 2014). Rainwater harvesting is the collection and accumulation of rainwater and runoff water, and water provision required for domestic consumption through vegetable-animal production (Oweis et al., 2001; Kantaroğlu 2009). Rainwater collected by pipes from open areas such as roads, sidewalks, and parking lots, especially on residential roofs, is filtered and then stored in the tank and this water is stored in garden irrigation, car washing, toilet reservoir, cleaning works, etc. can be used for needs (Eren et al., 2016; SFR, 2017). As a result of the collection, storage, and use of rainwater in this way, both water resources are protected, and economic gain is obtained.

The use of rainwater to meet alternative water needs is of great importance in water-saving and the protection and sustainability of water resources. When we look at the rain harvesting studies in the world, many concrete cisterns have been built in Thailand since the eighties, and the water collected here is used for drinking and use (Kılıç and Babuş, 2018). In the United States of America, approximately 250,000 houses have rainwater harvesting systems (Alparslan et al., 2008). In some islands in the Caribbean, a rainwater collection system is included in new structures (İncebel 2012). The use of gray water treatment systems or rainwater collection systems in buildings larger than 30,000 m² in Japan has been made mandatory by the Japanese Ministry of Public Works (Kılıç and Babuş, 2018). According to DIN (1989), in Germany, standards for rainwater collection systems, planning, installation, implementation and maintenance, rainwater filtration, rainwater reservoirs, and additional components are discussed (Sturm et al., 2009). New York World Trade Center. In this skyscraper, rainwater is collected on the roof and stored for irrigation of the surrounding park and cooling of this building, which saving 25% in energy used in building cooling (Tıkansak, 2013; Tanık, 2017). Frankfurt Airport Terminal B is used for rainwater, irrigation, and toilet washing. Germany Marburg Tennis Court is irrigated with rainwater supplied from outside (Tanık, 2017). In the United States, it is known that there are rainwater storage systems in 100,000 homes. It is known that most of these are for garden irrigation and plant growth, and 20% of them are for drinking water. (Dorak, 2015; Tanık, 2017). There are various examples of rainwater harvesting technology from building roofs in our country. Many technologies related to water conservation have been developed in the "Green Building Concept" in the Siemens Gebze Organized Industrial Zone. Rainwater collected from the roof can

be used in the fire irrigation system, softened and used as utility water in the whole area, and used in landscape irrigation outside the building. The rainwater collected from the roofs and coming to the water tank in Diyarbakır Solar House and the water obtained from domestic wastewater treatment are used in garden irrigation and toilet reservoirs by passing through a carbon filter. Rainwater collected from roofs at Borusan Oto İstinye Facilities is collected and treated in separate tanks and used in toilet reservoirs, vehicle washing, garden irrigation, and fire depot (Şahin and Manioğlu, 2011). Overall Turkey's examples regarding the use of rainwater, which is water-saving strategies to reduce water consumption in buildings, are seen as quite limited.

This study, it was aimed to investigate the potential of rainwater that can be collected from building roofs for irrigation of green areas in Mersin University Çiftlikköy campus and to determine its usability for greenfield irrigation needs. In this context, building roofs were detected by using multi-spectral UAV images to detect roof areas of the building. The object-based classification method has been used in the determination of building roofs.

With the development of technology, data collection methods have also improved, and especially image-based data have started to provide more detailed information in it (Demirel, 2010; Kavzaoğlu and Çölkesen, 2010; Demir, 2012; Kaya, 2020; Arasan et al., 2020; Saritur et al., 2020). The density of the data obtained made it necessary to infer the meaningful ones in these data. Previously, the extraction of the desired details was done manually by the operators. This extraction and classification process, which has been done manually for many years, has become faster and easier thanks to the developing detail extraction methods.

If pixel-based approaches are applied to obtain information from remotely sensed data, only spectral information is used. Therefore, pixel-based approaches cannot meet high-resolution image classification and information extraction is based solely on gray level thresholding methods, requiring the user to deal with big data. In this case, the pixel-based classification method applied in high-resolution images with rich information content, buildings, roads, parks, etc. Precise data extraction from urban areas with strict boundaries makes it very difficult. This deficiency has brought along advanced image analysis and classification approaches depending on the existing computing technologies. Therefore, in today's image processing and remote sensing technologies, object-based classification approaches have been used extensively (Baatiz et al., 2004; Bacher and Mayer, 2005; Marangoz, 2009; Bilgilioğlu, 2015; Yiğit and Uysal, 2019a; Yiğit and Kaya, 2020).

An object according to the object-based classification approach; is defined as a group of pixels with similar spectral and spatial properties. In this approach, segments representing objects; shape, texture, neighborhood relationship, morphological relations, area, height value, distance, geometric shape, standard deviation, density, and so on. It is analyzed

using values and assigned to target classes. Most of this information is specific to the object-based classification method, they cannot be used in the pixel-based classification method. More accurate classification results are obtained by using different properties of the object (Hofmann and Jain, 1987).

Kabadayı and Uysal (2020) detected buildings using high-resolution UAV images. They first subjected the digital products they produced from the UAV data to the segmentation process and then classified them using various indexes. Karlı et al. (2010), aimed to automatically extract building details from infrared aerial photographs. They pointed out that when it comes to object detection, segmentation is of great importance in image processing and computer vision techniques. Therefore, three different segmentation methods were used to extract building and road details. In their work, they revealed that building details can be determined automatically from infrared aerial photographs. Grigillo and Kanjir (2012) aimed to automatically extract buildings in cities and cities in an object-based manner in their study. They produced Normalized Digital Surface Model (nSYM) by producing Digital Surface Model (DSM) and Digital Terrain Model (DTM) produced from Lidar and digital images. The object-based classification method was chosen, and they preferred the multi-resolution segmentation method.

Kalkan and Maktav (2010) compared the object and pixel-based classification methods they made on satellite images. Since pixel-based classification is based only on the statistical analysis of pixels, they grouped the pixels in the segmentation stage and mentioned that these segments give more meaningful and positive results for the thematic class in the object-based classification method, which uses many properties such as color, frequency, and neighborhood. As a result of the study, they compared object and pixel-based classification methods. They stated that both pixel and object-based gave success results, and they obtained better results in high-resolution images thanks to the segmentation process used in the object-oriented classification method.

Firat and Erdoğan (2015) carried out an automatic detail extraction study by using multispectral aerial photographs and DSM and DTM in the object-based classification method. In the scope of the study, automatic extraction of vegetation cover and water surface details, especially the building, was examined. They used the height model and the Normalized difference vegetation index (NDVI) index for object extraction. It has been observed that the values entered by the operator just before the segmentation stage, which is the most important stage in object-based classification, affect the accuracy. For example; It was stated that the extraction of buildings was a success of

81%, and the buildings that could not be detected were small buildings and the reason for this was the scale parameter. As a result, it was stated that automatic object extraction from aerial photographs with object-based classification method was successful but using images with multispectral bands alongside SAM and DEM data would increase accuracy.

Since high-resolution UAV images are used in this study, the object-based classification method was preferred. In addition, since a large part of the study area consists of low green areas and forest areas, UAV images with Near-infrared (NIR) band have also been used, which contributes to higher accuracy in determining green areas.

Green areas, buildings, and roads were determined by the object-based classification method from digital products (Orthophoto-DSM-DTM) produced from images with Red-Green-Blue-NIR-Rededge (R-G-B-NIR-Redge) bands taken by UAV. Thanks to automatic detail detection, data clutter has been eliminated and the analysis process in large areas has become easier. After the determined buildings, the building roof areas were calculated. Then, the total amount of rainwater was calculated, and it was also investigated that what percentage of the irrigated green areas would be covered by rainwater if irrigated every day, once a week, and twice a week.

2. STUDY AREA

Mersin University located in Mersin city has nine campuses. Çiftlikköy Central Campus, the main campus site, was built in 1992. Çiftlikköy Campus, 14 kilometers away from the city center, has an area of 4 181 097 m². (Fig. 1).

A great deal of campus area is vegetated land and natural environment. University Administration takes measures in preserving natural habitat and forests. Mersin University gives priority to increasing the total forest area (1 363 873 m²) and planted vegetation area. In the current state, the area of vegetation that needs to be irrigated is 319552 m² while the built-up area (roof area of buildings) in total is 125 427 m² derived from UAV data. The rest of the campus area is designed and used for sports fields, pavements, and parking. Mersin University master plan aims to preserve natural habitat and water-absorbing land as one of the pillars of green campus planning. In this manner, limited development is planned for buildings and built-up areas.

Çiftlikköy Campus is among the privileged campuses with its original architectural design (Demirci & Özdemir, 2020) and contemporary arrangements, large and eye-catching buildings, green and forest areas, many social, cultural and sports facilities. It is one of the attractive campus sites in Turkey.



Figure 1. The Study area (White polygon shows the boundry of Mersin University)

3. MATERIEL and METHOD

Digital products were produced using images taken with a UAV belonging to the campus area. With these, buildings were automatically detected with the object-oriented classification approach. The UAVs used in the study for this purpose and technical information are given in Figure 2, Table 1 and 2, respectively.

A total of 1808 photographs were collected with the Parrot Bluegrass UAV from a height of 80 meters from a rare location and double grid (Figure 3). With the Sensefly + UAV, a total of 842 photographs were collected from a height of 120 meters from a rare location and overlapped (double grid).



Figure 2. UAV (A: Sensefly Ebee Plus UAV and S.O.D.A Camera B: Parrot Bluegrass UAV and Parrot Sequoia+ Camera)

Table 1. Parrot Bluegrass UAV and Parrot Sequoia + Camera basic technical features (Paksoy teknik, 2020a)

Specialty	Value
weight	1810 g
cruising speed	2-20 m/s
Max of flight time	About 25 minutes
Radiolink distance	2 km
Satellite Positioning Systems	+
Camera model	Parrot Sequoia+
Sensor type	R-G-Redge-NIR (14 mp)
4 x sensors Focal length	3.98 mm
RGB Focal length	4.88 mm

Table 2. Sensefly Ebee Plus UAV ve S.O.D.A Camera basic technical features (Paksoy teknik, 2020b)

Specialty	Value
Weight/ Size	1100 g /1100 mm
Cruising speed	40-110 m/s
Max of flight time	About 50 minutes
PPK/RTK	+
Radiolink distance	3 km
Satellite Positioning Systems	+
Sensor type/ Sensor size	R-G-B (20 mp)/ 1-inch
Resolution/ Focal Length	5472x3648/10.6 mm

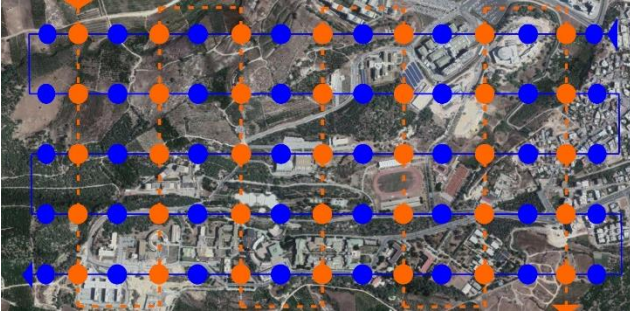


Figure 3. Double Grid Flightpath (Line: Flight Path – Circle: Sample photos) (UAV flight software: Emotion software for Ebee Sensefly, Pix4D Capture software for Parrot Bluegrass).

Besides, ground control points (GCP) were measured with a Global Navigation Satellite Systems (GNSS) device to bring the photogrammetric products obtained within the scope of the study to the same location as the ground location (Şasi & Yakar, 2018; Ulvi et al., 2020). Using these surveyed GCPs, digital maps have been brought to their real position (Spatial referencing has been made). For this process, a total of 32 YKNs, 20 of which are ground-centered in the campus and 12 on buildings and similar high-rise buildings, have been founded and measured.

3.1. Photogrammetric Process

Photogrammetry is a technique used to create digital maps that allow obtaining reliable measurements and information of physical objects by recording, measuring, and interpreting photographs or images obtained with metric cameras or unique sensor systems (Kraus, 2011).

One of the methods adopted in recent years to collect the spatial data needed is UAVs. With UAV technology, data of large areas can be collected faster and at a low cost. To produce a digital map of Mersin University Çiftlikköy Campus, flights were made with an MS sensor (Red-Green-Rededge-NIR) UAV and RGB (red-GreenBlue) sensor UAV. First of all, GCPs have been placed on the land to ensure that the obtained products coincide with the actual land location.

The images collected with the UAV are orientated with photogrammetric valuation software (Pix4d Mapper). At the end of the orientate, it was converted into a national coordinate system using GCPs measured from the field. Later, the orthophoto of the study area, DSM and DTM were produced.

In the study, since the rainwater to be collected on the roof building's roofs will be calculated and to obtain more precise location and height information, homogeneous distribution in the GCP facility was emphasized. A total of 32 GCPs were installed within the campus boundaries, 20 of which were installed at the ground center and 12 on the building's roofs. According to the terrain model, double grid flight planning was done by flying the MS sensor UAV from 80 meters. A total of 12 flights were carried out in the study area, and 1808 photographs were taken. Also, flights were made with an RGB sensor UAV from 120 meters, and 842 photographs were taken in 6 flights in total.

3.2. Object-Based Images Analysis

Object-oriented image analysis method; the shape, color, texture, etc. in the image analyze specific properties. It provides a system that captures objects according to their distinctive features (Bilgilioglu, 2015). This method: provides the ability to distinguish various objects in the image such as buildings, trees, roads, and vehicles. The object-based classification method includes segmentation and classification stages (Bergsjö, 2014). While the segmentation process allows the target classes on the image to be collected in the same segment, the second stage requires the classification of objects (Yiğit and Uysal, 2019a).

The most important and first step in object-based classification is segmentation.

Segmentation is the process of grouping pixels with similar spectral properties and creating image objects. The purpose of segmentation is to divide the image into different subsections and create meaningful objects (Baatz et al., 1999; Yiğit and Uysal, 2019b).

There are various segmentation methods in the literature. In this study's multi-resolution segmentation algorithm, image objects are divided into small pieces based on average heterogeneity for a given resolution. The heterogeneity criterion must be below a certain threshold. Weight parameters determine color and shape heterogeneity.

Color shape and compactness parameters are necessary for good image segmentation. Also, the scale parameter is required to stop the optimization process. The difference in heterogeneity is calculated before joining two adjacent objects. When the increment exceeds the threshold set by the scale parameter, the object join process is stopped and the partitioning is completed.

In the multi-resolution segmentation algorithm, the parameters are set by the user. These parameters are scale, color/shape, and softness/density. The parameters should be entered as close to the truth as possible. The most important of the 3 parameters entered is the scale parameter. The softness/density and Color/shape parameters complement each other to 1.

The Color and Shape criteria generate image objects consisting of relatively homogeneous pixels using the general Segmentation Function (SF) formulated in equation (1).

$$Sf = w_{color} h_{color} (1 - w_{color}) h_{shape} \quad (1)$$

where the user-defined weight for spectral color or shape is $0 < w_{color} < 1$.

Spectral (i.e., color) heterogeneity (h) of an image object is computed as the sum of the standard deviations of spectral values of each layer (σ_k) (i.e., band) multiplied by the weights for each layer (w_k):

$$h = \sum_{k=1}^m w_k \cdot \sigma_k \quad (2)$$

The color criterion is computed as the weighted mean of all changes in standard deviation for each band k of the m bands of remote sensing dataset. The standard deviation is σ_k weighted by the object sizes n_{ob} (i.e. the number of pixels):

$$h_{color} = \sum_{k=1}^m w_k [n_{mg} \cdot \sigma_k^{mg} - (n_{ab1} \cdot \sigma_k^{ab1} + n_{ab2} \cdot \sigma_k^{ab2})] \quad (3)$$

(where mg means merge).

Compactness:

$$c_{pt} = \frac{l}{\sqrt{n}} \quad (4)$$

Smoothness:

$$smooth = \frac{l}{b} \quad (5)$$

(Karakış et al., 2006)

n is number of pixels in the object, l is the perimeter, b is shortest possible border length of a box bounding the object

$$h_{cpt} = n_{mg} \cdot \frac{l_{mg}}{\sqrt{n_{mg}}} - \left(n_{ob1} \cdot \frac{l_{ab1}}{\sqrt{n_{ab1}}} + n_{ab2} \cdot \frac{l_{ab2}}{\sqrt{n_{ab2}}} \right) \quad (6)$$

$$h_{smoth} = n_{mg} \cdot \frac{l_{mg}}{b_{mg}} - \left(n_{ob1} \cdot \frac{l_{ab1}}{\sqrt{n_{ab1}}} + n_{ab2} \cdot \frac{l_{ab2}}{\sqrt{n_{ab2}}} \right) \quad (7)$$

$$h_{shape} = w_{cpt} \cdot h_{cpt} + (1 - w_{cpt}) \cdot h_{smoth} \quad (8)$$

After the images were separated into meaningful segments, each segment's properties were tested, and the responses of each feature in each image band and image segment were analyzed. The analysis led to the determination of the boundary values that would best represent the class based on the feature that captured the associated class distinction.

Thus, the classification continued with the limits set in the relevant membership function, and this stage was made cyclically until the best classification representing real-world conditions was obtained.

The software has two basic classifications. These are fuzzy membership and nearest neighborhood functions. In the nearest neighbor classification function, the user defines classes using sample objects for each class. In the fuzzy membership classification function, the ranges of the properties of objects belonging to a specific class or where they do not belong are defined.

In the classification phase, values belonging to the building-green area-road class were determined first. Then, classes were created by determining the properties of objects that do not belong to these classes. It was seen that some segments were assigned to the wrong class after the assignments to the classes were delayed. Merge and border reshaping operations were applied after the segments assigned to the wrong classes were assigned to the correct class. The indices used in the classification process are shown in Table 3. In the study, four class assignments were made with object-based classification as buildings, green areas, roads, and others.

Finally, an accuracy analysis was conducted to determine the compatibility of the classes with the real space. Accuracy analysis is the last step in measuring the accuracy and reliability of the classification. In order to check the classification quality and accuracy, the most common accuracy estimation parameters, general accuracy, manufacturer accuracy, user accuracy, and Kappa coefficient, were calculated using the TTA mask-based error matrix approach (Lu et al., 2004). TTA is a file called training and testing area mask that contains information about the classes created, allowing them to transfer existing samples to other scenes (Yiğit and Uysal, 2020). Building data obtained by geodetic methods were used as reference data sources (Base map made using GNSS and Total Station).

Table 3. RGB- Rededge-NIR band indices used in this study

Name	Index Name	Formula	Reference
GRVI	Green-red vegetation index (The Synthetic NDVI)	$\frac{(Green - Red)}{(Green + Red)}$	Motohka et al., 2010
RRI	Red ratio index	$\frac{(Red)}{(Blue + Green + Red)}$	Çömert et al., 2017
GRI	Green ratio index	$\frac{(Green)}{(Blue + Green + Red)}$	Sonntag et al., 2012
CBR	Common Band Ratio	$\frac{Blue + Green + Red}{3}$	Çömert et al., 2017
NDVI	Normalized Difference Vegetation Index	$\frac{NIR - Red}{NIR + Red}$	Rouse Jr et al., 1974
DDVI	Difference Difference Vegetation Index	$[(2 \times NIR - Red) - (Green - Blue)]$	Eisfelder, 2009
TDVI	Transformed Difference Vegetation Index	$1.5x \frac{NIR - Red}{\sqrt{NIR^2 + R + 0.5}}$	Bannari et al., 2002
$NDVI_{Rec}$	Red-edge NDVI	$\frac{NIR - Rededge}{NIR + Rededge}$	Gitelson and Merzlyak, 1994

3.3. Rainwater Efficiency Calculation

The Calculations for how much rainwater will be collected from the roof surface are summarized below (Eren et al., 2016; Kılıç and Abuş, 2018; Tema 2020).

Roof area: a functional area (m²) where rainwater can be collected.

Precipitation amount: It is the total annual precipitation amount determined by the General Directorate of Meteorology.

Roof coefficient (Yield Coefficient): German standards specify the coefficient as 0.8 in DIN (1989). The roof coefficient means that all the rain falling on the roof cannot be recycled. Filter efficiency coefficient: The coefficient specified by German standards as 0.9 in DIN (1989). The filter efficiency coefficient is the efficiency coefficient of the first filter passed to separate rainwater obtained from the roof from visible solids. It is a coefficient given by calculating that some water cannot pass through here. As a result, it is calculated by the formula below.

$$Rainwater_{harvesting} (m^3) = \frac{roof}{area} \times \frac{roof}{coefficient} \times \frac{filter}{efficiency} \times coefficient \times \frac{Precipitation}{amount} \left(\frac{mm}{year} \right) \quad (9)$$

$$Rainwater_{harvesting} (m^3) = \frac{roof}{area} (m^2) \times 0.9 \times 0.8 \times \frac{Precipitation}{amount} \left(\frac{mm}{year} \right) \quad (10)$$

4. RESULT and DISCUSSION

4.1. Photogrammetric Process

As a result of the images obtained with the Multispectral UAV and RGB UAV, ortho-mosaics belonging to the R, G, B, Red edge, NIR bands of the study area were produced. Besides, DTM and DSMs belonging to the region were obtained. The Ground Sample Distance (GSD) of orthophotos produced has a resolution of 2.7 cm. What is the mean, the real terrain equivalent of the distance between the centers of adjacent pixels in digital images is called GSD. The orthophoto and digital surface model (DSM) of the study area are shown in Figure 4.

In addition, Digital Terrain Model (DTM) was produced with Virtual Surveyor software. In this software, an orthophoto of the area and any DSM map are required to produce DTM. With these maps, points for the DTM map are generated automatically or manually. Then, a DTM map is obtained with these points.

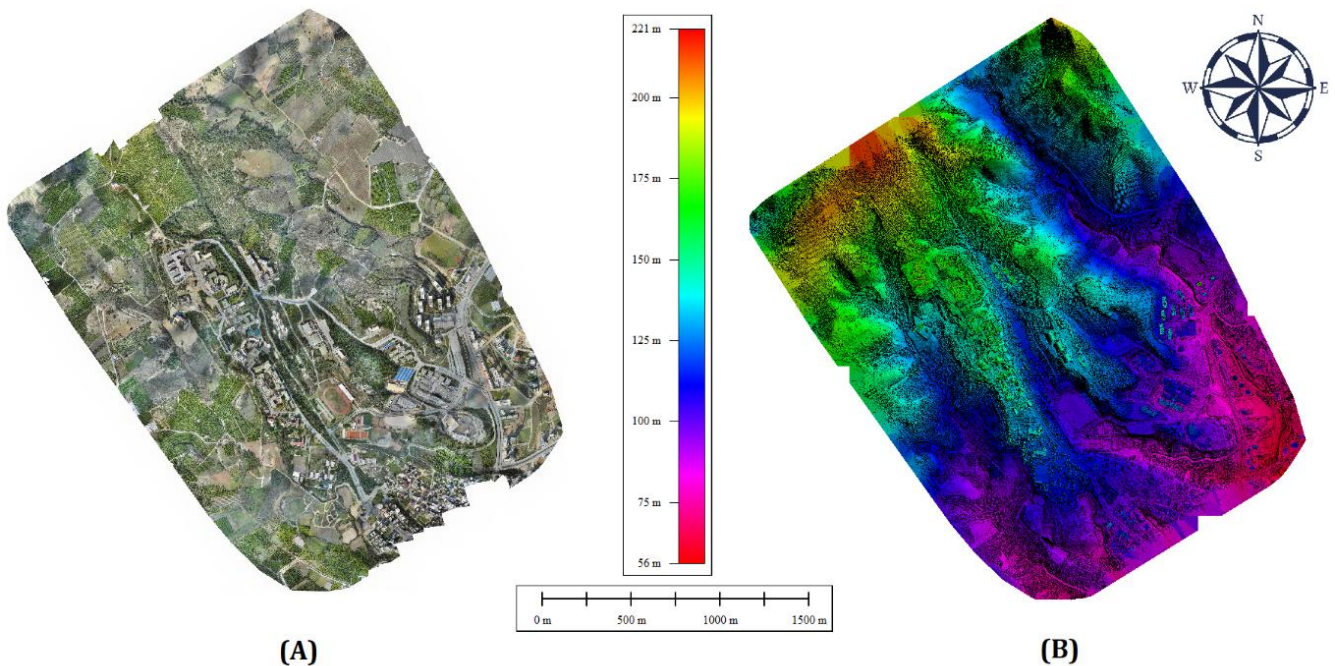


Figure 4. Digital map of the study area (A) Orthophoto (B) DSM

4.2. Detection of building roof areas

After producing digital maps (Orthophoto-DSM-DTM), the nDSM (Normalized digital surface model), the most preferred input product in building extraction, was first created. DSM-DTM formula is applied for the nDSM model.

After the digital maps were produced (Orthophoto-DSM-DTM-nDSM), the detailing extraction was started in the Definiens eCognition software. First, the segmentation process was applied to create meaningful objects from digital images. Before starting the

segmentation process, scale, softness/density, and color/shape parameters were determined. These three parameters entered in the segmentation stage were tried under different criteria, and 120 were selected for scale parameter, 0.6 for compactness parameter, and 0.4 for shape parameters. The segmentation result, according to the selected parameters, is shown in Figure 5.

After the segmentation process, the detail extraction and classification process was initiated. See Table 3 to look at the indices used in the classification process, and the classes created are shown in Figure 6.

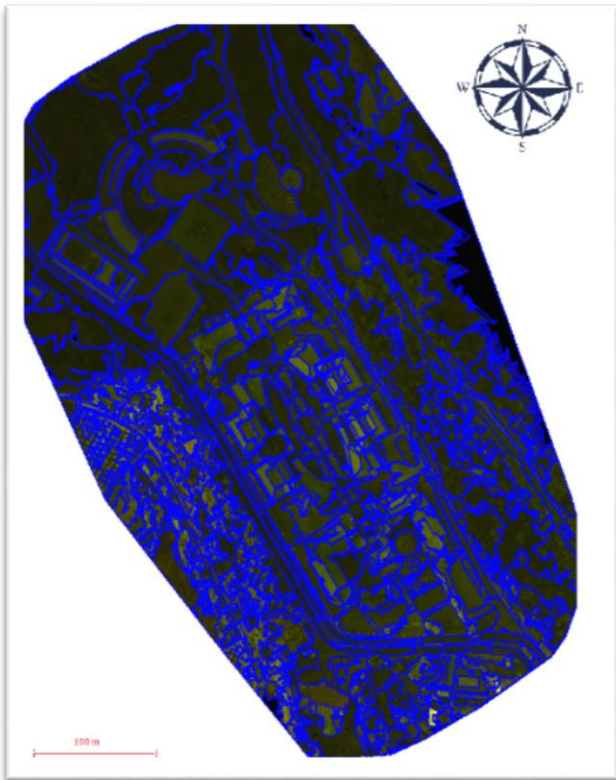


Figure 5. Segmentation result product (Sample area: Engineering faculty)

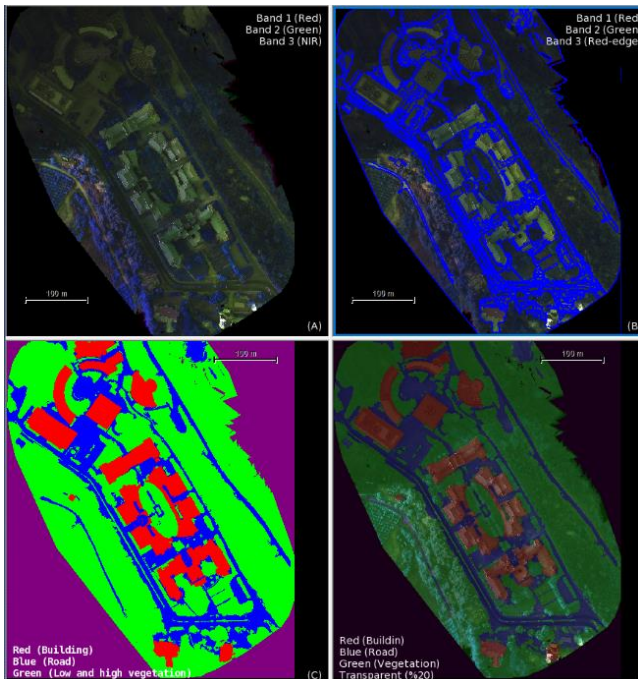


Figure 6. Classification steps for engineering faculty which is one of the sample areas. A: Input data, B: merged segmentation, C, and D: Classification results.

After the classification process, to check the classification quality and accuracy (for building roofs), the accuracy estimation parameters, general accuracy, manufacturer accuracy, user accuracy, sensitivity, originality, and Kappa coefficient were calculated (Table 4). Building data obtained by geodetic methods were used as reference data sources.

Table 4. Accuracy assessment by the TTA mask and random points analysis

General Accuracy	Producer Accuracy	Users Accuracy	Precision	Specificity	Kapa
0.919	0.872	0.859	0.916	0.893	0.904

With the object-based classification method, buildings are automatically detected quickly and with high accuracy. Finally, building roof boundaries have been simplified with the "Simplify Building" command in the GIS (Geographic information system) software (Arcgis) to generalize product data. Buildings where rain harvesting is possible and areas that need irrigation are shown in figure 7.

Eren et al. (2016) aimed to investigate the use potential of rainwater collected from building roofs in their university studies. Using the map drawing program, the total roof areas of the buildings and the size of the green areas in each zone were calculated. However, within the scope of the study, no details were given about the provision of digital data on building roofs. Roofs of buildings may have been obtained from existing projects, digital plan data, or digitization from platforms such as Google Earth.

Utsav et al. (2014) constitutes another example of a university. The study was carried out at Sankalchand Patel University Visnagar campus. In the study, it was mentioned that the total basin area was calculated and data for all the buildings of the campus were collected. But the method is not specified. In this study too, there is no information about how data on buildings and roofs are obtained.

Building roofs were detected using high-resolution UAV (in the study) or satellite imagery (Hacar, 2020; Orhan & Yakar, 2016) data without the need for any plan or digital data. In our study, unlike the literature, the data of the buildings were obtained from high-resolution images without using any plan data. In this way, the potential for rain harvesting of large zone or areas can be easily determined and a new perspective has been given to rain harvesting studies on building roofs.

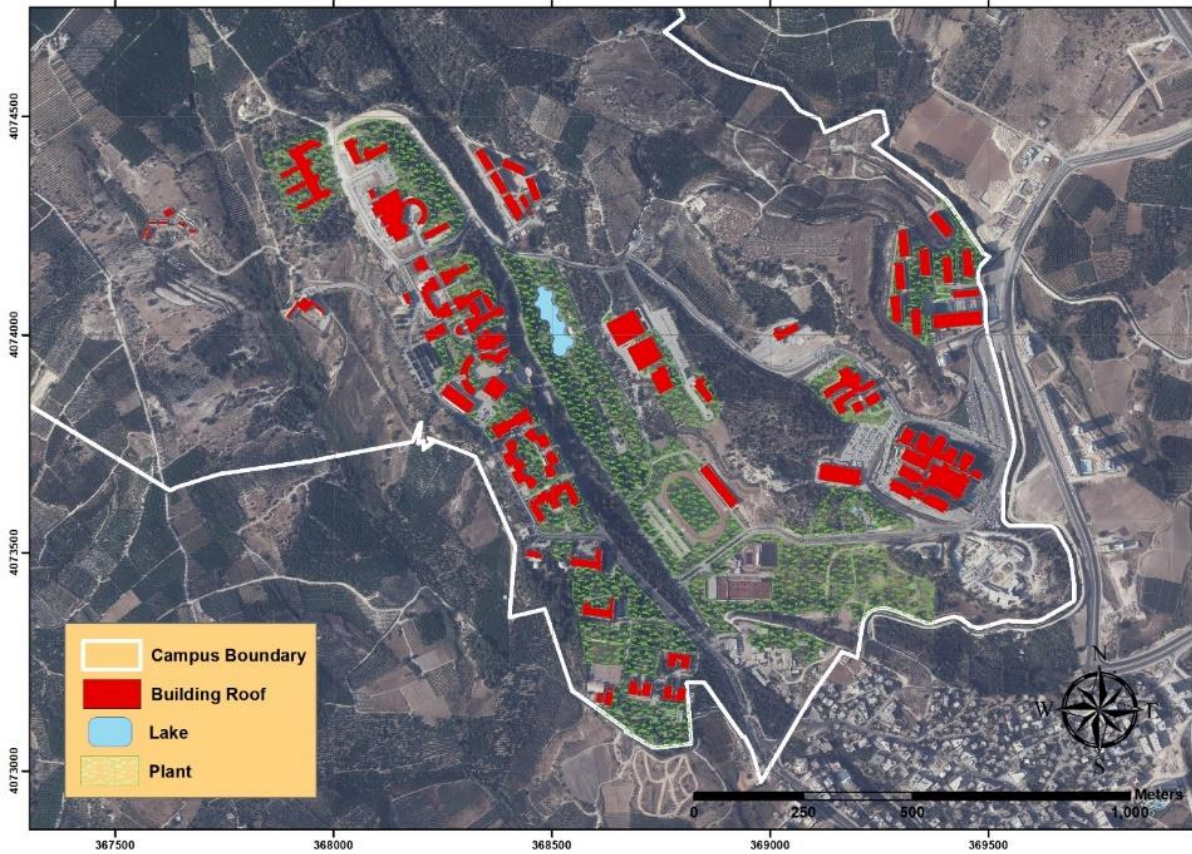


Figure 7. Roof areas suitable for rain harvesting and irrigated green areas.

4.3. Rainwater harvest

The last 30 years' data of the meteorology station located in the study area was obtained from the Turkish State Meteorological Service, and accordingly, it was seen that the annual rainfall was 655 mm (655 l/m²). In addition, as a result of the object-based classification process, the roof area of the buildings within the campus boundaries was determined as 125 427 m².

Rainwater harvesting:

$$125\,427\text{ m}^2 \times 655\text{ l/m}^2 \times 0.8 \times 0.9 = 59\,151\,373\text{ L} \\ = 59\,151\text{ m}^3/\text{year}$$

4.4. Calculation of the amount of water required for green field irrigation;

Considering the diversity of vegetation in the campus, it was found that although there are trees, there are generally leafy shrub and grass. In addition, considering the irrigation areas, it was determined that most of them were leafy shrub and grass. The irrigation need of leafy shrub is 8.25 mm / day (8.25lt / m²), and the irrigation need of grass is 7.25 mm / day (7.25lt / m²) in hot climatic regions (Erdoğan, 2002). Since it is known that the shrub and grass are of equal density, this

value is taken as 7.75 mm / day (7.75 l / m²) for the working area.

The green areas within the campus boundaries were extracted as a result of the Object-based classification process. However, during the field study, it was noticed that not all these areas were irrigated or that certain areas (forest) did not need irrigation. For this reason, only the green vegetation (leafy shrub and grass) areas where irrigation is carried out were corrected with the help of local measurements. As a result of the correction, the irrigation areas within the campus boundaries were determined as 319 552 m².

The daily amount of water for irrigation:

$$319\,552\text{ m}^2 \times 7.75\text{ l/m}^2 = 2476528\text{ l} = 2477\text{ m}^3/\text{day}$$

Irrigation water needs are calculated separately for cases where irrigation is done every day, twice a week and once a week, and are given in Table 5. It has been determined that the amount of water collected from the roof areas will meet 6.5% of the total garden irrigation water if irrigation is done every day, 23% of the total garden irrigation water if irrigation is done twice a week, 45.8% of the total garden irrigation water if irrigation is done once a week.

Table 5. Irrigation needs and efficiency values according to different irrigation periods

Amount of rainwater collected (m ³ /year)	The daily amount of water for irrigation (m ³)	once every day		twice every week		once every week	
		Total water requirement (m ³)	Percentage of water met (%)	Total water requirement (m ³)	Percentage of water met (%)	Total water requirement (m ³)	Percentage of water met (%)
59 151	2 477	904 105	6.5	258316	23	129 158	45.8

5. CONCLUSION

In this study, rainwater as an alternative water resource was emphasized and information about rainwater harvesting was given. In addition, the roof areas were automatically extracted using the object-based classification method with the help of UAV data. This situation sets an example for extracting building areas at the regional, district or local scale and easily determining the region's total rainwater harvesting potential.

In the Mersin University rainwater harvesting study, 59 151 m³ / year usable rainwater is obtained from the roofs of the existing 125 427 m² buildings. It has been demonstrated that the collected rainwater can be saved up to 46% if the water need of 319 552 m² of green area, which is irrigated regularly in the campus, is met once every week.

70% of the water consumed for drinking and utility purposes is used for toilets, garden irrigation, car-washing and laundry. Only 30% of the rainwater goes into groundwater, and the remaining 70% goes directly into the sewage. Considering the importance of water for living things, it becomes clear how important it is to evaluate rainwater (Eren et al., 2016; Kılıç and Abuş, 2018). Considering the results obtained from the study, it is seen that storing rainwater and using it in green area irrigation is of great importance in terms of sustainable use of existing water resources and saving water. By extending these systems, ecological balance will be preserved, sustainable development will be ensured, and water resources will be used more efficiently. For this reason, the importance of collecting and using rainwater in buildings should be explained to all members of society, and every individual should be encouraged in this regard.

ACKNOWLEDMENT

This study was supported by Mersin University Scientific Research Projects Coordination Unit (Project Number:2020-1-AP5-3836).

REFERENCES

Alparslan N, Tanık A & Dölgen D (2008). Türkiye’de Su Yönetimi Sorunlar ve Öneriler. Türk Sanayicileri ve İşadamları Derneği (TÜSİAD) Yayın No: T/2008-09/469. Ankara

Arasan G, Yılmaz A, Fırat O, Avşar E, Güner H, Ayğın K, Yüce D (2020). Accuracy Assessments of Göktürk-1 Satellite Imagery. *IJEG*, 5 (3), 160-168.

Baatz M & A Schäpe (1999). Object-oriented and multiscale image analysis in semantic networks. In: Proc. Of the 2nd International Symposium on Operationalization of Remote Sensing, August 16th-20th, Enschede. ITC.

Baatz M, Benz U, Dehghani S, Heynen M, Höltje A & Hofmann R (2004). eCognition Professional: User Guide 5, Definiens-Imaging, Munich.

Bacher U & Mayer H (2005). Automatic road extraction from multispectral high resolution satellite images. *IAPRS*, 36, Vienna, Austria, August 29-30, 2005.

Bannari A, Asalhi H & Teillet P M (2002). Transformed difference vegetation index (TDVI) for vegetation cover mapping. In IEEE International geoscience and remote sensing symposium (Vol. 5, pp. 3053-3055). IEEE.

Bergsjö J (2014). Object based change detection in urban area using KTH-SEG. Bachelor Thesis, Kth Royal Institute Of Technology, Stockholm.

Bilgilioğlu B B (2015). Uzaktan algılanmış görüntülerden faydalınalarak nesne tabanlı sınıflandırma yöntemi ile kent merkezlerindeki detayların çıkarımı ve yorumlanması. Yüksek Lisans Tezi, Aksaray Üniversitesi, Fen Bilimleri Enstitüsü, Aksaray, 79.

Çömert R, Matcı D K, Avdan U (2017). Yıkılmış Binaların Nesne Tabanlı Sınıflandırma ile İnsansız Hava Aracı Verilerinden Tespit Edilmesi, 4. Uluslararası Deprem Mühendisliği ve Sismoloji Konferansı, Eskişehir.

Demir İ (2012). Hadoop tabanlı büyük ölçekli görüntü işleme altyapısı. Yüksek Lisans Tezi, Kocaeli Üniversitesi, Fen Bilimleri Enstitüsü, 87.

Demirci Ş, Özdemir C (2020). Anechoic Chamber Measurements for Circular Isar Imaging at Mersin University’s Meatr Lab. *IJEG*, 5 (3), 150-159.

Demirel A Ş (2010). Sayısal görüntü arşivi bilgi sistemi. Doktora tezi, Selçuk Üniversitesi, Fen Bilimleri Enstitüsü, 96.

DIN (1989). Regenwassernutzungsanlagen. Deutsches Institut Normung DIN: 1989, German.

Dorak S (2015). Nilüfer Çayı ve Nilüfer Çayı'na deşarj edilen kimi arıtma tesisi atık sularının sulama suyu kalite parametrelerinin belirlenmesi (Master's thesis, Uludağ Üniversitesi).

Eisfelder C, Kraus T, Bock M, Werner M, Buchroithner M F & Strunz G (2009). Towards automated forest-type mapping—a service within GSE Forest Monitoring based on SPOT-5 and IKONOS data. *International Journal of Remote Sensing*, 30(19), 5015-5038.

Erdoğan O (2002) Kocaeli İli Sahil Düzenlemesinin Sulama Sistemi Projelendirilmesi, Yüksek Lisans Tezi. İstanbul Üniversitesi Fen Bilimleri Enstitüsü Peyzaj Mimarlığı Ana Bilim Dalı, İstanbul, 55 s.

Eren B, Aygün A, Likos S & Damar A İ (2016). Yağmur Suyu Hasadı: Sakarya Üniversitesi Esentepe Kampüs Örneği. 4th International Symposium on Innovative Technologies in Engineering and Science 3-5November 2016 (ISITES2016 Alanya/Antalya - Turkey)

Fırat O & Erdoğan M (2015). Nesne (Obje) Tabanlı Sınıflandırma Tekniği İle Multispektral Hava Fotoğraflarından Otomatik Bina Çıkarımı, Tufuab VII. Teknik Sempozyumu 21-23 Mayıs 2015, Konya

Grigillo D & Kanjir U (2012). Urban object extraction from digital surface model and digital aerial images, *ISPRS Annals of the Photogrammetry, Remote Sensing and Spatial Information Sciences*, 3, 215-220, Melbourne, Australia

Hacar M (2020). A Rule-Based Approach for Generating Urban Footprint Maps: From Road Network to Urban Footprint. *IJEG*, 5 (2), 100-108.

- Haddeland I, Heinke J, Biemans H, Eisner S, Flörke M, Hanasaki N & Stacke T (2014). Global water resources affected by human interventions and climate change. *Proceedings of the National Academy of Sciences*, 111 (9), 3251-3256.
- Hoffman R & Jain A K (1987). Segmentation and classification of range images. *IEEE Transactions on Pattern Analysis and Machine Intelligence*, 9, 608-620.
- Paksoy teknik (2020a). http://www.paksoytekni.com.tr/images/paksoy-topcon/iha/parrot_bluegrass, [Access: 01.05.2020].
- Paksoy teknik (2020b). <http://www.paksoytekni.com.tr/images/PAKSOY-TOPCON/IHA/sensefly>, [Access: 01.05.2020].
- İncebel C (2012). Alternatif su kaynaklarının endüstriyel kullanıma kazandırılması için çatı yağmur suyu hasadı (Ostim örneği). Yüksek Lisans Tezi, Gazi Üniversitesi Fen Bilimleri Enstitüsü, Ankara.
- Kabadayı A & Uysal M (2020). Çok yüksek çözünürlüklü İHA verilerinden bina tespiti. *Türkiye İnsansız Hava Araçları Dergisi*, 2 (2), 43-48.
- Kalkan K & Maktav D (2010). Nesne Tabanlı Ve Piksel Tabanlı Sınıflandırma Yöntemlerinin Karşılaştırılması (İkonos Örneği), II. Uzaktan Algılama ve Coğrafi Bilgi Sistemleri Sempozyumu, 11 - 13, Gebze - KOCAELİ.
- Kantaroglu Ö (2009). Yağmur suyu hasadı plan ve hesaplama prensipleri. IX. Ulusal Tesi Mühendisliği Kongresi, 6-9 Mayıs, İzmir.
- Karlı F, Fidan M H & Dihkan M (2010). Kızılötesi Hava Fotoğraflarından Bina Detaylarının Çıkarılması. III. Uzaktan Algılama ve Coğrafi Bilgi Sistemleri Sempozyumu, 11-13, Gebze - KOCAELİ.
- Kavzoğlu T & Çölkesen İ (2010). Destek vektör makineleri ile uydu görüntülerinin sınıflandırılmasında kernel fonksiyonlarının etkilerinin incelenmesi. *Harita Dergisi*, 144 (7), 73-82.
- Kaya Y (2020). Çok bantlı uydu görüntüleri kullanılarak buğday bitkisinin incelenmesi – Ceylanpınar TİGEM örneği. Yüksek Lisans Tezi, Harran Üniversitesi, Fen Bilimleri Enstitüsü, 84.
- Kılıç M Y & Abuş M N (2018). Bahçeli Bir Konut Örneğinde Yağmur Suyu Hasadı. *Uluslararası Tarım ve Yaban Hayatı Bilimleri Dergisi*, 4(2), 209-215.
- Kılıç S (2008). Küresel İklim Değişikliği Sürecinde Su Yönetimi. İ.Ü. Siyasal Bilgiler Fakültesi Dergisi, 39, 161-186.
- Kraus K (2011). *Photogrammetry: geometry from images and laser scans*. Walter de Gruyter.
- Lu D, Mausel P, Brondizio E & Moran E (2004). Change detection techniques. *INT. J. REMOTE SENSING*, 25 (12), 2365-2407.
- Marangoz A M (2009). Uydu görüntülerinden kentsel ayrıntıların nesne-tabanlı sınıflandırma yöntemiyle belirlenmesi ve cbs ortamında bütünleştirilmesi, Doktora tezi, Yıldız Teknik Üniversitesi, Fen Bilimleri Enstitüsü, İstanbul, 133.
- Motohka T, Nasahara K N, Oguma H & Tsuchida S (2010). Applicability of green-red vegetation index for remote sensing of vegetation phenology. *Remote Sensing*, 2, 2369-2387.
- Olaniyi O A, Olutimehin I.O & Funmilayo O A (2019). Review of climate change and its effect on Nigeria ecosystem. *International journal of Rural Development, Environment and Health Research*, 3 (3).
- Orhan O & Yakar M (2016). Investigating land surface temperature changes using Landsat data in Konya, Turkey. *International Archives of Photogrammetry, Remote Sensing and Spatial Information Sciences*, 41, 285-89.
- Oweis T & Prinz Dand Hachum A (2001). Water Harvesting: Indigenous Knowledge for The Future of The Drier Environments. International Center for Agricultural Research in the Dry Areas (ICARDA), Aleppo, Syria.
- Rouse Jr J W, Haas R H, Deering D W, Schell J A & Harlan J C (1974). Monitoring the Vernal Advancement and Retrogradation (Green Wave Effect) of Natural Vegetation.
- Şahin N & Manioğlu G (2011). Binalarda yağmur suyunun kullanılması. *Tesi Mühendisliği*, 125: 21-32.
- Sandalcı M & Yüksel İ (2011). İklim Değişikliğinin Türkiye'deki Göller ve Barajlar Üzerindeki Etkisi, *Yapı Dünyası Dergisi*, 181, 25 - 29, 2011.
- Saritur B, Bayram B, Duran Z, Seker D (2020). Feature Extraction from Satellite Images Using Segnet and Fully Convolutional Networks (FCN). *International Journal of Engineering and Geosciences*, 5 (3), 138-143.
- Şasi A & Yakar M (2018). Photogrammetric modelling of hasbey dar'ülhuffaz (masjid) using an unmanned aerial vehicle. *International Journal of Engineering and Geosciences*, 3 (1), 6-11.
- SFR (2017). Yağmur suyu filtreleme ve depolama sistemi. <http://www.sfr.com.tr/yagmur-suyu-hasati-s6.html> [Access: 08.11.2020].
- Sonnentag O, Hufkens K, Teshera-Sterne C, Young A M, Friedl M, Braswell B H & Richardson A D (2012). Digital repeat photography for phenological research in forest ecosystems. *Agricultural and Forest Meteorology*, 152, 159-177.
- Sturm M, Zimmermann M, Schutz K, Urban W & Hartung H (2009). Rainwater harvesting as an alternative Water resource in rural sites in central northern Namibia. *Physics and Chemistry of the Earth*, 34: 776-785.
- Tanık A (2017). Yağmur Suyu Toplama, Biriktirme ve Geri Kullanımı (Doctoral dissertation, Yüksek Lisans Tezi, İTÜ İnşaat Fakültesi, Çevre Mühendisliği Bölümü).
- Tema (2020). TEMA-Geleceğin suyu. http://sutema.org/resources/Document/FileName/2015-12-01_22-11-14-692%20GeleceginSuyu.pdf [Access: 15.11.2020].

Tıkansak T E (2013). Konutlarda enerji etkinliği. <https://www.tse.org.tr/Icerik/HaberDetay?HaberID=13010> [Access: 19.11.2020].

Trenberth K E (2011). Changes in precipitation with climate change. *Climate Research*, 47 (1-2), 123-138.

Ulusoy K (2007), Küresel Ticaretin Son Hedefi: Su Pazarı, Kristal Kitaplar Yayınevi,

Ulvi A, Yakar M, Yiğit A Y & Kaya Y (2020). İHA ve Yersel Fotogrametrik Teknikler Kullanarak Aksaray Kızıl Kilise'nin 3 Boyutlu Nokta Bulutu ve Modelinin Üretilmesi. *Geomatik Dergisi*, 5 (1), 22-30.

Utsav R P, Vikrant A P, Manjurali I B & Harhad M R (2014). Rooftop Rainwater Harvesting (RRWH) at SPSV Campus, Visnagar: Gujarat - A Case Study.

IJRET: International Journal of Research in Engineering and Technology, 3 (4), 821-825

Yiğit A Y & Kaya Y (2020). Sentinel-2A uydu verileri kullanılarak sel alanlarının incelenmesi: Düzce örneği. *Türkiye Uzaktan Algılama Dergisi*, 2(1), 1-9.

Yiğit A Y & Uysal M (2019a). Nesne tabanlı sınıflandırma yaklaşımı kullanılarak yolların tespiti. *Türkiye Fotogrametri Dergisi*, 1 (1), 17-24.

Yiğit A Y & Uysal M (2019b). Nesne Tabanlı Sınıflandırma ile Taşkın Alanlarının Analizi. *Resilience*, 3(2), 369-385.

Yiğit A Y & Uysal M (2020). Automatic road detection from orthophoto images. *Mersin Photogrammetry Journal*, 2 (1), 10-17.



© Author(s) 2020. This work is distributed under <https://creativecommons.org/licenses/by-sa/4.0/>